Meteorol. Z. (2001), **122**, pp. 1–999

Testing broadband radiation schemes for their ability to calculate the radiative forcing and temperature response to stratospheric water vapour and ozone changes

By P. M. de F. FORSTER[1] *, M. PONATER[2] and W. Y. ZHONG[3]

[1] *University of Reading, U.K.*

[2] *DLR Oberpfaffenhofen, Germany*

[3] *Imperial College, U.K.*

(Revised draft 11-7-01)

Zusammenfassung

Aus beobachteten nderungen (1979-1997) von Kohlendioxid sowie stratosphrischem Wasserdampf und Ozon wurden mit verschiedenen Strahlungsmodellen sowohl der Strahlungsantrieb als auch die stratosphrische Temperaturnderung unter Verwendung der Nherung unvernderter dynamischer Erwrmungsraten (fixed dynamical heating) berechnet. Es zeigt sich, dass Breitband-Strahlungsschemata den instantanen Strahlungsantrieb von stratosphrischem Wasserdampf um bis zum 50knnen. Fr den adjustierten Strahlungsantrieb (stratosphrische Temperaturnderungen bercksichtigend) betrgt die Unterschtzung etwa 15reduziert die zugehrige stratosphrische Abkhlung und 30hat zur Folge, dass auch der adjustierte Strahlungsantrieb durch stratosphrisches Ozon um bis zu 50Der Fehler kann durch Aufspaltung der wichtigsten Absorptionsbande fr Wasserdampf in zwei separate Banden korrigiert werden. Diese Arbeit unterstreicht die Notwendigkeit sorgfltiger berprfung eines Strahlungsschemas, wenn damit zustzliche (ursprnglich nicht vorgesehene) Strahlungsantriebe abgeschtzt werden sollen.

Abstract

The radiative forcing and fixed dynamical heating temperature response is calculated for observed

* Corresponding author: Piers Forster, Department of Meteorology, University of Reading, PO Box 243, Earley Gate, Reading, Berkshire, RG6 6BB, UK.

changes (1979-1997) in carbon dioxide, stratospheric ozone and stratospheric water vapour, using several radiation schemes. It is found that certain broadband schemes substantially underestimate the radiative forcing and absorption by stratospheric water vapour by up to 50%, for the instantaneous forcing, and 15% for the adjusted radiative forcing. This error in the water vapour absorption leads to a 30% smaller stratospheric temperature response and also causes an underestimate of the adjusted stratospheric ozone radiative forcing of up to 50%. It was found that this error could be corrected by splitting the wavelength band which accounts for strong water vapour absorption into two separate bands. This work illustrates the need to carefully test each new forcing introduced into a broadband scheme, as its designer may not have catered for such eventualities.

1. Introduction

To enable a general circulation model (GCM) to correctly respond to changes in radiatively active gases it is important that the radiation scheme employed can correctly model the radiative forcing and the heating rate changes induced by a change in a given atmospheric constituent. As well as errors in the radiation scheme, there are often significant errors in the model climatology which may also impact on the radiative forcing, calculated for a given perturbation. This paper discusses to which extent radiative forcing results are affected by such errors, taking as examples some frequently used radiation schemes.

A combination of stratospheric ozone depletion, carbon dioxide increases, and possible increases in stratospheric water vapour may have led to some of the largest changes to the Earth's energy balance in recent decades (Forster and Shine, 1999). These climate forcings are also believed to be largely responsible for the observed cooling in the lower stratosphere over a similar time period (WMO, 1999). As a GCM's temperature response in the stratosphere is similar to that from using the fixed dynamical heating approximation (e.g. Rosier and Shine, 2000), it is a useful exercise to compare the radiative temperature response from the broadband models, employed in GCM's for their speed, with more sophisticated models. Errors in a given GCM's stratospheric temperature response and radiative forcing will directly affect its ability to attribute the observed temperature changes to a particular cause.

2. Methodology

This paper compares radiative forcing and fixed dynamical heating (FDH) temperature response calculations from the Reading Narrow Band Model (NBM) with two broadband schemes, based on versions of the Morcrette (1991) radiative transfer code. A previous comparison of ozone radiative forcing calculations found considerable differences of up to 30% between radiative transfer schemes (Shine *et al.*, 1994). This paper tests models which were not involved in the earlier ozone forcing comparison and investigates their agreement for stratospheric water vapour forcing calculations. The three main schemes employed in this paper are briefly described below.

ECHAM: (Roeckner et al., 1996) This version of the Morcrette (1991) scheme has updated ozone absorption cross sections and is used in the ECHAM4 General Circulation Model, where, for example, it has been used to estimate ozone radiative forcings (e.g. Ponater *et al.*, 1999) and the climate response to ozone changes (e.g. Bengtsson *et al.*, 1999).

ZHONG: (Zhong *et al.*, 1996) This is based on Morcrette (1991). It contains updates to the water vapour continuum as well as the water vapour and ozone absorption cross sections, both at solar and thermal wavelengths. It is used in the Reading Intermediate General Circulation Model (IGCM); it has also been used to calculate the radiative forcing and stratospheric temperature response for stratospheric water vapour and ozone changes (e.g. Smith *et al.*, 2001).

NBM: (Shine, 1991, Forster and Shine, 1997). This has been used extensively in the calculation of radiative forcing for well mixed greenhouse gases (e.g. Myhre *et. al* 1998) and ozone (Forster and Shine 1997); it has been found to calculate radiative forcings and heating rates which agree to within roughly 10% of those from more sophisticated line by line models. However, it is over 1000 time slower than the broadband schemes, described above.

Each of these models have been set up to take exactly the same input atmosphere, fixing the vertical levels at which irradiances and heating rates are calculated. Clouds are specified in terms of their altitude and liquid water path and radiative forcings are calculated at the height of the tropopause, using the World Meteorological Organization lapse rate definition (WMO, 1986). A 25 level zonally and seasonally averaged 5°latitude resolution input climatology of ozone, water vapour, temperature and cloud is used as the basis for the radiative calculations. This climatology is described in Christidis *et al.*, (1997). The adjusted radiative forcing and stratospheric temperature response are calculated using the fixed dynamical heating (FDH) approximation (Ramanathan and Dickinson, 1979). This approximation is a way of calculating the change in stratospheric temperatures by assuming that the dynamical heating at a given height and latitude remains fixed at its unperturbed value. The experiments are outlined below.

CO2: A 31 ppmv increase in carbon dioxide, from its 1979 value of 336 ppmv.

OZONE: The 1979-1997 seasonal ozone trends from Randel and Wu (1999) were used. These trends were added to the seasonal climatology above its tropopause.

WSTRAT: A simple increase of 0.7 ppmv in water vapour above the tropopause, as used in Forster and Shine (1999) to approximate the observed trend over the 1979-1997 period.

WTROP: A 10% increase in tropospheric water vapour mixing ratio, used for testing purposes only.

3. Comparison of instantaneous radiative forcings

Figure 1 shows the annually and globally averaged shortwave (SW) and longwave (LW) instantaneous radiative forcings from the various experiments, assuming a background atmosphere of the most important radiatively active gases (H_2O, CO_2, O_3, CH_4 and N_2O) and clouds. Clouds were included as they have a considerable effect on the ozone and carbon dioxide forcings. However, they were found to have only a minimal influence (2%) on the differences between the radiation schemes. For an explanation of the sign of the calculated radiative forcings the reader is referred to IPCC (1995).

It can be seen that the models give instantaneous radiative forcings, for the CO2, WTROP and OZONE experiments, which all agree to within roughly 10% of each other. This excellent agreement of the instantaneous ozone radiative forcings, particularly in the SW are an considerable improvement over an earlier comparison of ozone radiative forcings (Shine *et al.*, 1994) which found differences in the ozone radiative forcing of up to 30% in the SW and 20% in the LW, between different models. Differences in the LW have also improved mainly due to all the models including ozone absorption in its 14 micron band, which several models in the earlier comparison did not employ.

However, for WSTRAT the LW forcing from the ZHONG and ECHAM schemes are over 40% lower than the NBM model. There is also a considerable difference between the SW forcing in the ECHAM model and the other two models - compounding the difference in its net radiative forcing. The larger SW water vapour absorption, in the ECHAM code, has also been observed in earlier versions of Morcrette-based radiation codes (Morcrette, 1990).

The fact that the tropospheric LW water vapour forcings are in such good agreement between the models means that the differences in the WSTRAT forcing are not due to general differences in the water vapour absorption characteristics of the models. An analysis of the variation with wavelength of the WSTRAT LW forcings showed that 90% of the forcing originates from 0-500cm^{-1}. This region is divided into 2 bands in the Morcrette (1991) based codes, with nearly all of the difference in radiative forcing (80%) coming from the strong water vapour band of the Morcrette based scheme (in which a single band includes absorption in both the 0-350cm^{-1} and 1450-1880 cm^{-1} regions).

To test in which of the radiation schemes an error may lie, several LW radiative transfer schemes were used to calculate the instantaneous radiative forcing for a 0.7 ppmv increase in stratospheric water vapour. These experiments assumed an annually and globally averaged clear-sky water vapour only atmosphere. The radiative forcings and downwards irradiance at the tropopause are shown in Table 1. It can be seen that the schemes which are not based on Morcrette (1991) agree within 5% of the line by line model. However, the Morcrette (1991) based schemes all underestimate the downwards irradiance and the radiative forcing by as much as 45%. Modifications were made to the ZHONG radiation scheme to test possible reasons for this underestimation, results from these two models are also shown in the Table. ZHONG-2 uses a look up table of the line-by-line model pre-computed transmittances to find the water vapour absorption in the strong water vapour band. ZHONG-3 went one stage further, and not only used a table of pre-computed transmittances, but also split the strong water vapour band into the two regions 0-350cm^{-1} and 1450-1880 cm^{-1}. It can be seen that while the use of the lookup table gives a 9% higher forcing, the splitting of the band increases the LW forcing by some 21%. This increase in the radiative forcing brings the ZHONG-3 scheme into very good agreement with the line by line model result. These results illustrate that the two parts of the strong water vapour band are too different in their stratospheric water vapour absorption characteristics to be treated as a single entity. The reason why this difference manifests itself for stratospheric water vapour is that the water vapour amounts are several orders of magnitude smaller than in the troposphere, so the absorption is much more wavelength dependent, due to the water vapour bands not being as saturated.

4. Adjusted radiative forcing and stratospheric temperature response

Figure 2 shows the FDH temperature changes for the CO2, OZONE and WSTRAT experiments. Generally it can be seen that the three radiation schemes have similar patterns of temperature response. However, there are some noteworthy differences.

CO2: Both the ZHONG and the ECHAM scheme give a slight temperature increase below 15 km. This is not in evidence in the NBM scheme, which does not account for CO_2 absorption in the SW. When the ECHAM experiment was repeated to exclude SW absorption, no stratospheric heating was observed (see Figure 2). Above 40 km, where the ECHAM scheme is not designed to operate, the ZHONG scheme gives a greater cooling, due to the inclusion of Doppler broadening which is not simulated by the other models.

OZONE: There is remarkably good agreement between the radiation schemes, except in the 25-35 km region, where the ECHAM model gives a significant cooling, whereas the other two models show almost no change in temperature. This difference was found to be due to the effects of water vapour absorption and is discussed further below.

WSTRAT: Increases in stratospheric water vapour lead to a greater LW emission to space and hence a stratospheric cooling. As expected from the results of the previous sections the ECHAM and ZHONG schemes both substantially underestimate the FDH cooling due to stratospheric water vapour increases, by up to 40% at 16 km for the ECHAM model. However, the ZHONG-3 scheme with its split water vapour band is in very good agreement with the NBM.

It was speculated that the poor representation of stratospheric water vapour in the broadband models may affect their ability to model FDH temperature response to the CO2 and OZONE experiments. These experiments were therefore repeated excluding stratospheric water vapour from the atmosphere. Apart from an overall increased cooling little effect was found on the CO2 temperature response. However, for OZONE the differences between the models temperature change between 25-35 km were greatly reduced (to within 5%).

Figure 3 shows the adjusted radiative forcings for the CO2, OZONE and WSTRAT experiments. For all the scenarios the cooling of the stratosphere, observed in Figure 2, reduces the downwards LW irradiance at the tropopause, making the LW radiative forcing more negative (for OZONE) or less positive (for CO2 and WSTRAT) than the instantaneous values in Figure 1. For the OZONE experiment differences between the models have grown to over 20% as the NBM has a larger change in the downwards LW for a given temperature change, which makes the LW adjusted radiative forcing more negative. The differences in the LW forcing have a proportionally much larger effect on the net radiative forcing: the net NBM forcing is twice as negative as the ECHAM forcing and 30% more negative than the ZHONG forcing. These differences were found to be largely due to the extra absorption by stratospheric water vapour in the NBM. If stratospheric water vapour is removed from the radiation schemes their net adjusted radiative forcings were found to be within 12-25% of each other and the LW forcings within 5% (see Figure 3).

In a similar fashion to the OZONE experiments, the WSTRAT experiment in the NBM also has a larger change in the downwards LW irradiance, due to stratospheric temperature adjustment. However, as the NBM instantaneous LW forcing was more positive than the other two, the extra forcing change due to adjustment brings the ZHONG and ECHAM WSTRAT net forcings to within 15% and 30% of the NBM forcing respectively. The inclusion of the split water vapour band into the ZHONG-3 scheme can be seen to reproduce radiative forcings within 10% of the NBM.

5. GCM CLIMATOLOGY ERRORS

As well as the somewhat simplified radiation schemes employed in GCMs they invariably have differences between their long term climatology and observations. These differences could be expected to impact on radiative forcing and stratospheric temperature response calculated within the GCM framework. In this section differences between the ECHAM4 model climatology and the observationally-based climatology are used to illustrate the effect on radiative forcing of changes in the background profile. The effect of differences in temperature, ozone and water vapour were examined. For a discussion of these differences and their possible reasons the reader is referred to Roeckner *et al.*, (1996).

Water vapour: The observationally based climatology used water vapour derived from Stratospheric Aerosol and Gas Experiment II (SAGE II) and Halogen Occultation Experiment (HALOE) satellite measurements above 300 hPa. Between 300 hPa and the surface European Centre for Medium Range Weather Forecasts (ECMWF) analysis data is used. In the troposphere ECHAM water vapour mixing ratios are within 10% of the climatology. In the lower stratosphere the ECHAM model has roughly 1 ppmv (30%) lower values than the climatology.

Temperature: The observational data is based on ECMWF analysis, see Christidis *et al.*, (1997) for further details. Model to observation differences were dominated by a mid and high latitude (above 30°) cold bias at the tropopause in the ECHAM model which extended down to about 5 km. This cold bias is quite marked, having a maximum of more than 10 K at 200 hPa. In the rest of the atmosphere the ECHAM model is roughly 1-2 K warmer than the observations.

Ozone: The observational climatology is based on a 1985-1990 average of satellite and ozonesonde data (Li and Shine, 1995). The prescribed monthly averaged ozone distribution in the ECHAM model generally agreed to within 20% of the climatology. The largest differences were found in the high latitude lower stratosphere, where the ECHAM model had 30% higher ozone mixing ratios, possibly due to some ozone depletion in the climatology.

To test the effect of these differences on the calculated radiative forcing, the temperature, ozone or water vapour in observational climatology were replaced by their equivalent in the ECHAM4 model and the radiative forcing calculations repeated.

Figure 4 shows the differences in the NBM adjusted radiative forcing obtained by employing different background profiles. It can be seen that even relatively large changes in the temperature, ozone and water vapour profiles generally alter the net radiative forcing by no more than a few percent for all but two of the experiments. Most of these differences were found to be due to the effect of background profile changes on the stratospheric temperature adjustment, which was only slightly altered.

The exceptions were found for changes to the ozone and water vapour profiles in the OZONE and WSTRAT experiments respectively. These changes gave differences of over 10% for OZONE and were caused by changes in the stratospheric temperature adjustment. For the OZONE experiment with the perturbed ozone background slightly less cooling was found, making its net radiative forcing more positive. For WSTRAT, the instantaneous forcing depends strongly on the amount of water vapour in the background profile, as many of the water vapour lines are very strong and easily saturated, therefore the reduced water vapour in the ECHAM background profile increases the forcing by nearly 20%. However, these differences can still be deemed to be relatively small when compared to the current uncertainties in correctly specifying ozone and stratospheric water vapour trends (see e.g. WMO, 1999).

6. Discussion and conclusions

This paper has compared radiative forcings and stratospheric temperature response for carbon dioxide, stratospheric ozone and water vapour changes calculated by two broad-band and one narrow band scheme.

Combining water vapour absorption from the 0-350cm^{-1} and 1450-1880 cm^{-1} regions of the spectrum and errors in characterising the absorption characteristics in the Morcrette (1991) based radiation schemes were found to lead to an underestimate of absorption by stratospheric water vapour in the thermal infrared by as much as 30%. This deficiency manifests itself by causing a significant underestimate (>30%) of the instantaneous LW forcing and the stratospheric temperature response for a stratospheric water vapour change. Our results imply that calculations of the adjusted stratospheric water vapour radiative forcing, which employ a version of the ZHONG radiation scheme (e.g. Smith *et al.* 2001), may be underestimated by roughly 15%. Likewise, it is obvious now why the ECHAM4 model provided a comparatively small forcing for supersonic aircraft induced water vapour increase in the stratosphere (Prather and Sausen, 1999, their Table 6-4).

The instantaneous SW and LW OZONE forcings agreed to within 10% of each other. This represents a considerable improvement over a previous inter-comparison of ozone radiative forcing from different models (Shine *et al.*. 1994). However, the reduced stratospheric water vapour absorption in the ECHAM model was found to lead to a 50% less negative adjusted radiative forcing and a reduced stratospheric cooling in the OZONE experiment, than in the NBM. Radiative forcing differences using the ZHONG scheme were not so pronounced; however, the scheme still gave OZONE forcings approximately 30% less negative than the NBM. This means that stratospheric temperature responses and radiative forcings calculated, employing this type of scheme (e.g. Rosier and Shine, 2000, Smith *et al.* 2001) may have underestimated the effects of stratospheric ozone by an equivalent amount.

Using a typical GCM background climatology to calculate radiative forcings, rather than observations, also was found to lead to errors of up to 20% in the forcings examined. However, this error is small for carbon dioxide (2%) and, for stratospheric ozone and water vapour changes, considerably less than the uncertainty in the trends themselves.

The increase in stratospheric temperatures just above the tropopause for carbon dioxide changes was found to be caused by its SW absorption. It is therefore this SW absorption which may dictate the altitude of cross over between a heating and cooling for CO_2 changes. This cross-over altitude is important in the attribution of climate change problem (e.g. IPCC 1995).

Broad-band schemes in GCMs were never designed to model the effects of all possible climate forcings. This work illustrates the importance of extensively testing a GCMs radiation scheme for the calculation of each new forcing introduced.

Acknowledgements

PMF carried out this work while visiting DLR, he thanks them for their support; he was also funded by NERC grant GT5/99/AS/5. The two reviewers are thanked for helpful comments.

References

Bengtsson, L., Roeckner, E., Stendel, M. 1999 Why is the global warming proceeding much slower than expected? *J. Geophys. Res.-Atmos.*, **104,** 3865-3876

Christidis, N. 1999 Halocarbon radiative forcing in radiation and general circulation models *Ph.D Thesis*, University of Reading, U.K.

Christidis, N. Hurley, M. D. Pinnock, S. Shine, K. P. Wallington, T.J. 1997 Radiative forcing of climate change by CFC-11 and possible CFC- replacements *J. Geophys. Res.-Atmos.*, **102,** 19597-19609

Edwards, D. P. 1992 GENLN2: A general line-by-line atmospheric transmittance and radiance model. Version 3.0 description and user's guide. *Report NCAR/TN-367+STR.* NCAR, Boulder, CO, USA.

Edwards, J. M. and Slingo, A. 1996 Studies with a flexible new radiation code .1. Choosing a configuration for a large-scale model *Q. J. R. Meteorol. Soc.*, **122,** 689-719

Forster, P. M. de F. and Shine, K. P. 1997 Radiative forcing and temperature trends from stratospheric ozone changes *J. Geophys. Res.-Atmos* , **102,** 10841-10855

Forster, P. M. de F. and Shine, K. P. 1999 Stratospheric water vapour changes as a possible contributor to observed stratospheric cooling *Geophys. Res. Lett.* , **26,** 3309-3312

IPCC 1995 *IPCC, Climate Change 1994, Radiative forcing of climate change and an evaluation of IPCC IS92 emission scenarios* Cambridge University Press, Cambridge, U.K.

Kiehl, J. T., Hack, J. J. and Briegleb, B. P. 1994 The simulated Earth radiation budget of the National Center for Atmospheric Research Community Climate Model CCM2 and comparisons with the Earth Radiation Budget Experiment (ERBE) *J. Geophys. Res.-Atmos.*, **99,** 20815-20827

Li, D. and Shine, K. P. 1995 A 4-dimensional ozone climatology for UGAMP models *UGAMP Internal Report* , **35,** University of Reading, U.K.

Morcrette, J. J. 1990 Impact of changes to the radiation transfer parameterizations plus cloud optical-properties in the ECMWF model *Mon. Weather Rev.*, **118,** 847-873

Morcrette, J. J. 1991 Radiation and cloud radiative properties in the European Center for Medium Range Weather Forecasts forecasting system *J. Geophys. Res.-Atmos.*, **96,** 9121-9132

Myhre, G., Highwood, E. J., Shine, K. P. and Stordal, F. 1998 New estimates of radiative forcing due to well mixed greenhouse gases *Geophys. Res. Lett.*, **25,** 2715-2718

Ponater, M., Sausen, R., Feneberg, B. and Roeckner, E. 1999 Climate effect of ozone changes caused by present and future air traffic *Clim. Dyn.*, **15,** 631-642

Prather, M. and Sausen, R. 1999 Potential climate change from aviation *IPCC special report "Aviation in the Global Atmosphere"*, 185-215, Cambridge University Press, Cambridge.

Ramanathan, V. and Dickinson, R. E. 1979 The role of stratospheric ozone in the zonal and seasonal energy balance of the Earth-troposphere system *J. Atmos. Sci.*, **36,** 6831-6864

Randel, W. J. and Wu, F. 1999 A stratospheric ozone trends data set for global modelling studies *Geophys. Res. Lett.*, **26,** 3089-3092

Roeckner, E., Arpe. K., Bengtsson, L., Christoph, M., Dumenil, L., Esch, M., Giorgetta, M., Schlese, U. and U. Schulzweida 1996 The atmospheric general circulation model ECHAM4: model description and simulation of present day climate *Max Planck Inst. for Meterol. Rep. 218*, Hamburg.

Rosier, S. M. and Shine, K .P. 2000 The effect of two decades of ozone change on stratospheric temperature as indicated by a general circulation model *Geophys. Res. Lett.* , **27,** 2617-2620

Shine, K .P. 1991 On the cause of the relative greenhouse strength of gases such as the halocarbons *J. Atmos. Sci.*, **48,** 1513-1518

Shine, K .P., Briegleb, B. P., Grossman, A. S., Hauglustaine, D., Mao, H. Ramaswamy, V., Schwarzkopf, M. D., Van Dorland, R. and W.-C. Wang 1994 Radiative forcing sue to changes in ozone - a comparison of different codes *Atmospheric Ozone as A climate Gas, NATO ASI Series*, Springer-Verlag, Berlin

Smith, C. A., Haigh, J. D. and R. Toumi 2001 Radiative forcing due to trends in stratospheric water vapour *Geophys. Res Lett.*, **28,** 179-182

WMO 1986 *WMO, Scientific assessment of ozone depletion, 1998.* World Meteorological Organization, Global Ozone Research and Monitoring Project- Report No. 16, Geneva, Switzerland.

WMO 1999 *WMO, Scientific assessment of ozone depletion, 1998.* World Meteorological Organization, Global Ozone Research and Monitoring Project- Report No. 44, Geneva, Switzerland.

Zhong, W. Y., Toumi, R. and Haigh, J. D. 1996 Climate forcing by stratospheric ozone depletion calculated from observed temperature trends *Geophys. Res. Lett.*, **23,** 3183-3186

Figure 1. Instantaneous LW (top panel) and SW (bottom panel) radiative forcing (W/m^2) for the CO2, OZONE, WSTRAT and WTROP experiments. Results are for the three different radiative transfer schemes: NBM (black bar), ECHAM (dark grey bar) and ZHONG (light grey bar).

Figure 2. Shows the globally and annually averaged FDH stratospheric temperature response for the CO2 (top panel), OZONE (middle panel) and WSTRAT (bottom panel) experiments. Results are plotted for the three different radiative transfer schemes: NBM (thick solid line), ECHAM (dashed line) and ZHONG (dotted line). The top panel also shows the results of the CO2 experiment in the ECHAM model excluding the effects of SW absorption by CO_2 (thin solid line). The bottom panel also shows the results from using the ZHONG-3 scheme with its improved water vapour absorption (very thick solid line). Each panel indicates the line of zero temperature change (dot-dash line).

Figure 3. Adjusted LW (top panel) and net (bottom panel) radiative forcing (W/m^2) for the CO2, OZONE, WSTRAT and OZONE (excluding stratospheric water vapour) experiments. Results are shown for the three different radiative transfer schemes: NBM (black bar), ECHAM (dark grey bar) and ZHONG (light grey bar). The radiative forcing for the ZHONG-3 scheme is also shown for WSTRAT as an unfilled light grey bar

Figure 4. Percentage change in the adjusted net NBM radiative forcing from using a pertubed background profile, compared to an observationally based profile. Results are shown for the CO2, OZONE and WSTRAT experiments. Changes in the climatology are either made to the water vapour profile, temperature profile or ozone profile and are described in the text.

TABLE 1. MODEL COMPARISON OF STRATOSPHERIC WATER VAPOUR LW RADIATIVE FORCING.

Model	Dn Irrad. at trop. (Wm^2)	R. Forcing (Wm^2)
RFM	3.08	0.257
NBM	3.15	0.261
NCAR CRM	3.25	0.247
EDWARDS+SLINGO	3.10	0.244
CHRISTIDIS	3.10	0.250
ZHONG	2.61	0.207
ECHAM	2.22	0.178
MORCRETTE	2.43	0.191
ZHONG-2	2.90	0.225
ZHONG-3	3.20	0.272

Downwards longwave irradiance at tropopause and the radiative forcing for a 0.7 ppmv increase in stratospheric water vapour for a water vapour only atmosphere. Results are for the globally and annually averaged atmosphere using different radiative transfer schemes. RFM, a line-by-line model based on Edwards (1992); NCAR Community Radiation Model (Kiehl *et al.* 1992), EDWARDS+SLINGO: 9 band scheme (Edwards and Slingo 1996), CHRISTIDIS: (Christidis, 1999) A broadband scheme used in Forster and Shine (1999) to calculate stratospheric water vapour radiative forcings. ZHONG-2: as ZHONG, with the absorption in the strong water vapour band ($0\text{-}350 cm^{-1}$+$1450\text{-}1880\ cm^{-1}$) replaced by line-by-line pre-computed transmission tables. ZHONG-3: As ZHONG-2 with strong water vapour band split.

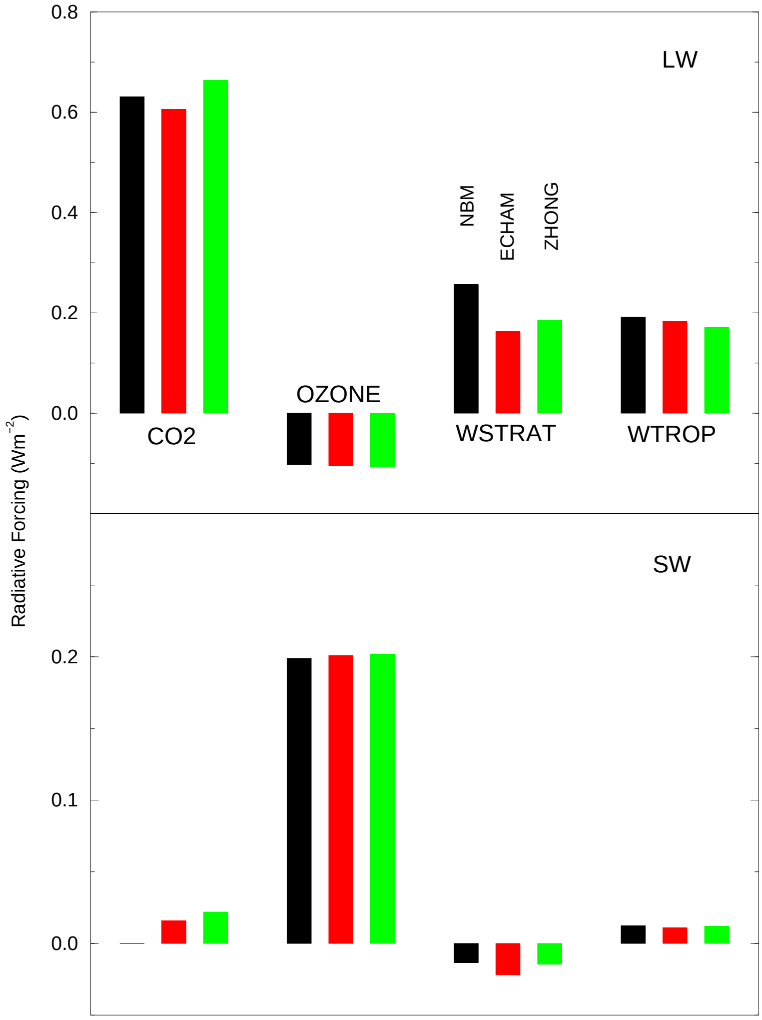
0.8
0.6
0.4
0.2
0.0
LW
NBM
ECHAM
ZHONG
CO2
OZONE
WSTRAT
WTROP
Radiative Forcing (Wm^{-2})
SW
0.2
0.1
0.0

Figure 1:

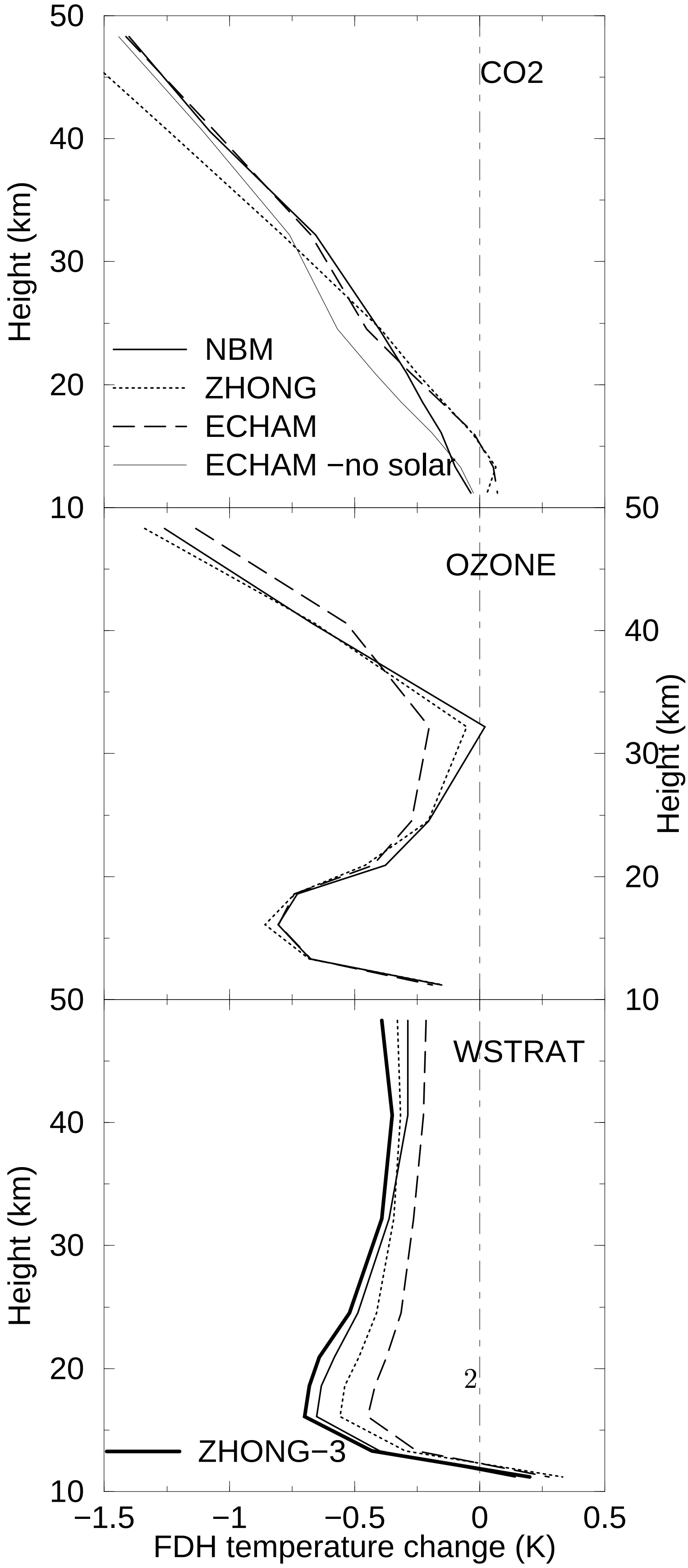

CO2
OZONE
WSTRAT
NBM
ZHONG
ECHAM
ECHAM −no solar
ZHONG−3
Height (km)
Height (km)
Height (km)
FDH temperature change (K)
−1.5
−1
−0.5
0
0.5
10
20
30
40
50
2

Figure 2:

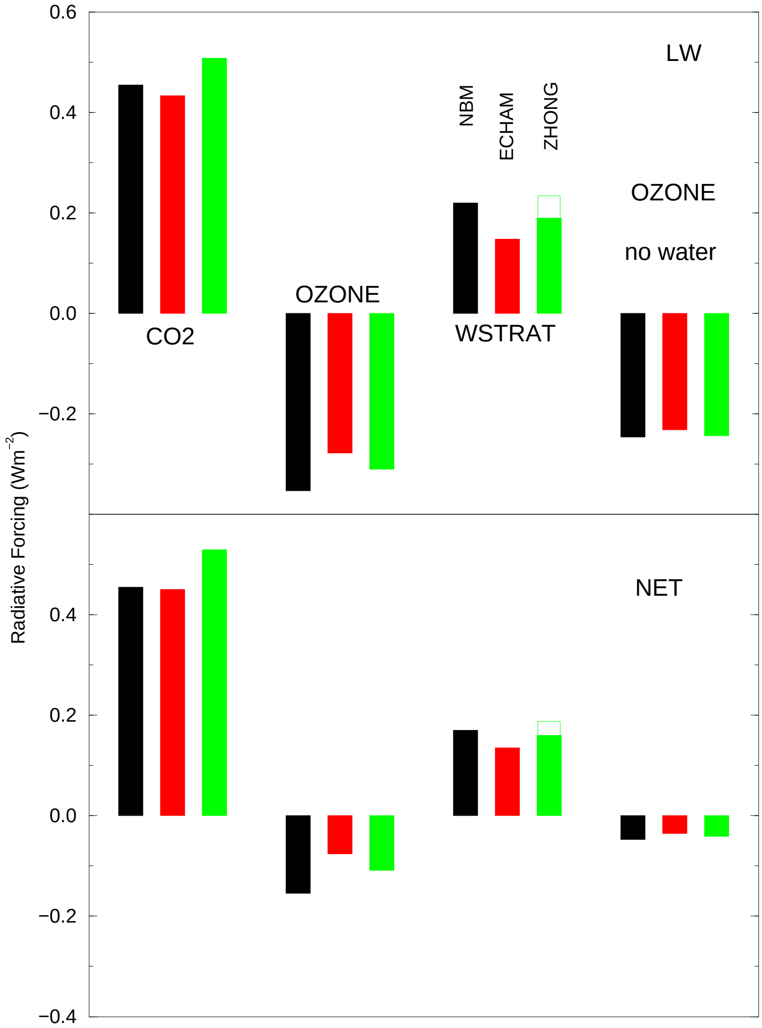

0.6
0.4
0.2
0.0
−0.2
LW
NBM
ECHAM
ZHONG
OZONE
no water
OZONE
CO2
WSTRAT
Radiative Forcing (Wm^-2)
NET
0.4
0.2
0.0
−0.2
−0.4

Figure 3:

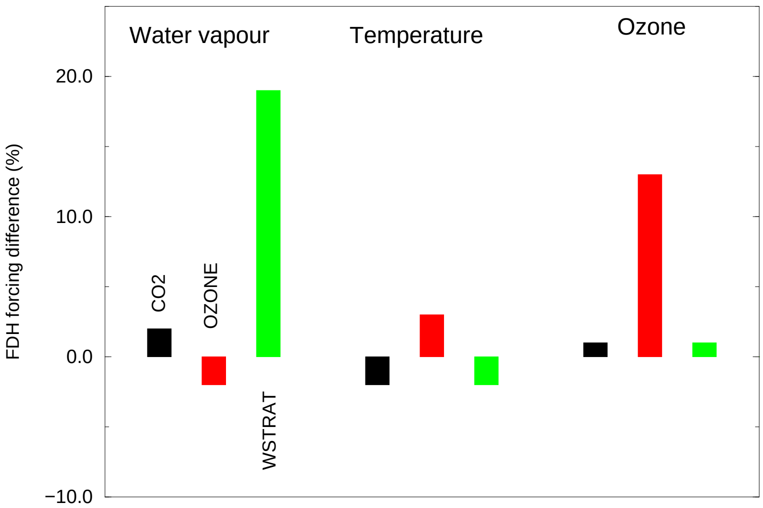
Water vapour
Temperature
Ozone
20.0
10.0
0.0
−10.0
FDH forcing difference (%)
CO2
OZONE
WSTRAT

Figure 4: